16TH EUROPEAN CONFERENCE ON EARTHQUAKE ENGINEERING THESSALONIKI 18 - 21 JUNE 2018

SEISMIC CAPACITY AND LIMIT STATE DEFINITION IN FRAGILITY ANALYSIS OF RETROFITTED BRIDGE PIERS

Sotiria STEFANIDOU[1], Andreas KAPPOS[2,3]

ABSTRACT

A number of analytical methodologies have been developed over the last three decades for the seismic assessment of bridges and the derivation of fragility curves for 'typical' bridges. Only very recently, the research focus has shifted on the derivation of bridge-specific fragility curves, recognising that seismic assessment is affected by different geometry, structural system, bridge component, and ground properties. In this context, a new, component-based methodology for the derivation of bridge-specific fragility curves was proposed by the authors (Stefanidou and Kappos, 2017); this methodology is extended here to retrofitted bridges, considering the effect of different retrofit properties on pier capacity and limit state definition.

The main issue addressed in this study is to determine through analysis the seismic capacity and limit state thresholds for retrofitted bridge piers, considering different common retrofit measures, namely reinforced concrete (R/C) jackets and FRP jackets. A range of different as-built and retrofitted component properties, i.e. a variety of geometry, material, reinforcement, axial load, and jacket properties are considered; parametric analysis is performed and empirical relationships for limit state thresholds definition of retrofitted bridge piers with R/C and FRP jackets are proposed. Finally, the methodology for the derivation of bridge-specific fragility curves is applied to a case-study bridge retrofitted with R/C and FRP jackets. The case study puts in context the importance of case-dependent (as per the selected retrofit scheme) limit state threshold definition in seismic fragility analysis.

Keywords: Bridges; Seismic assessment; Fragility analysis; Retrofitting; R/C jackets; FRP jackets

1. INTRODUCTION

Recognising the significant role of bridges as part of the transportation system during an earthquake event, detailed seismic design provisions for bridges were included in recent design codes worldwide, while several retrofit measures were developed for the enhancement of bridges' seismic performance concerning both the superstructure and substructure. The measures can be classified into those that target displacement control (restrainer cables, shear keys, seat extenders), strength and ductility enhancement (R/C, steel, or FRP jackets) and increase of energy dissipation (elastomeric or lead bearings, viscous dampers). The seismic performance of retrofitted bridge components was first evaluated after the 1994 Northridge earthquake, where significant damage occurred to older bridges, including some retrofitted, resulting in questioning the effectiveness of several retrofit measures and strategies used.

Taking into consideration the fact that the conceptual framework of seismic codes is the minimization of superstructure and substructure damage rather than total prevention of damage, numerous methodologies have been developed for the seismic vulnerability assessment of as-built and retrofitted bridges for different levels of seismic hazard, concerning both seismically and non-seismically designed bridges. The differences among the existing methodologies mainly lie in the quantitative definition of limit states (engineering demand parameter used, threshold values of limit states considered), the type

[1]Postdoctoral Researcher, Civil Engineering Department, Aristotle University of Thessaloniki, GR 54124, ssotiria@civil.auth.gr

[2]Professor, Civil Engineering Department, Aristotle University of Thessaloniki, GR 54124, ajkap@civil.auth.gr

[3]Director, Research Centre for Civil Engineering Structures, Civil Engineering Department, City, University of London, London, EC1V 0HB, UK, Andreas.Kappos.1@city.ac.uk

of analysis, the treatment of uncertainty and the probabilistic model used for fragility analysis (probabilistic seismic demand model, response surface models, 'metamodels') (Nielson, 2005, Towashiraporn, 2004). It should be underlined that the methodologies developed for retrofitted bridges are very few (Padgett and DesRoches 2009, Kim and Shinozuka, 2004), whereas the limit state thresholds proposed for the retrofitted components in terms of the selected engineering demand parameter (i.e. drift, curvature ductility) are not differentiated from the corresponding ones for as-built components, nor accounting for the effect of the properties of the specific retrofit measures (e.g. drift limits according to HAZUS recommendations are not differentiated for the case of R/C and FRP jacket). Since fragility is the probability that bridge damage exceeds a specific limit state threshold for a given level of earthquake intensity, the key issue for a reliable estimation is the qualitative and quantitative limit state definition (capacity), and the demand estimation. To this end, a new methodology was recently proposed by the authors (Stefanidou and Kappos, 2017), providing empirical relationships for component-specific limit state definition, two alternative procedures for demand estimation based on the desired level of accuracy and computational cost, and uncertainty treatment (uncertainties in capacity, demand and limit state definition are quantified). The main issue addressed herein, is the extension of the methodology to retrofitted bridges. Empirical relationships for the calculation of component-specific limit state thresholds (in terms of displacement) are proposed for piers retrofitted with different methods (R/C and FRP jackets). The effect of varying as-built and retrofitted pier properties on component capacity and limit state definition is presented and discussed, and the methodology is then applied to a case-study bridge, to derive fragility curves for the two alternative retrofit strategies (R/C and FRP jackets). The effect of component-specific limit state definition on fragility curves of retrofitted bridges is outlined, comparing the fragility curves from the proposed methodology to those derived considering limit state thresholds according to HAZUS recommendations (Mander and Basöz, 1999).

2. METHODOLOGY FOR THE DEVELOPMENT OF BRIDGE-SPECIFIC FRAGILITY CURVES FOR RETROFITTED BRIDGES

A new methodology for the development of bridge-specific fragility curves was recently proposed by the authors with a view to improving the reliability of loss assessment and prioritizing retrofit of the bridge stock. A detailed description of the methodology can be found elsewhere (Stefanidou and Kappos, 2017, Stefanidou, 2016); its key features are listed below, highlighting the ones relating to the extension to retrofitted bridges:

- Fragility of all critical components is accounted for in the estimation of the bridge system's fragility. Piers, bearings and abutments are considered as critical components, while series connection between components is assumed for the estimation of system fragility.
- Limit state (LS) thresholds for retrofitted components are qualitatively and quantitatively defined based on available experimental data and analysis results. Four limit states are considered, and component damage is defined in terms of local engineering demand parameters (EDPs) (such as curvature), while mapping of local to global EDPs (i.e. displacement of control point d_i) is performed using inelastic analysis results.
- A database of piers retrofitted with various techniques (i.e. R/C or FRP jacket) is created, considering a wide range of possible properties of as-built pier and retrofitted piers. Damage is initially defined in terms of *local* EDPs (i.e. curvature correlated with crack widths), mapped to *global* EDPs (i.e. displacement of component control point) via inelastic (pushover) component analysis, considering both flexural and shear failure modes. Analyses results are processed using the advanced least squares method and empirical relationships for component-specific LS threshold (d_i) values are provided for different pier types (circular and hollow circular piers) and retrofit measures (R/C and FRP jackets), considering the effect of as-built core and jacket properties on threshold values.
- Two alternative procedures (detailed and simplified) for demand estimation based on the desired level of accuracy and computational cost are proposed for seismic demand estimation at the control point of each component. The minimum requirements for the simplified procedure are the consideration of correlation between components, and of different boundary conditions at abutment location (open-closed gap).

- Uncertainties in capacity, demand, and limit state definition are quantified for retrofitted components and system assuming the distribution of key random variables, namely material strengths (core and jacket), ultimate concrete strain and plastic hinge length, gap size, bearings, and ground properties.
- Development of MATLAB-based software for the calculation of bridge-specific fragility curves for as-built and retrofitted bridges, that drastically reduces the time and effort required for the implementation of the proposed methodology to a large number of bridges within an inventory.

3. SEISMIC CAPACITY AND LIMIT STATE DEFINITION FOR RETROFITTED BRIDGE PIERS

As described in the previous section, the first step of the proposed component-based methodology for the development of bridge-specific fragility curves for retrofitted bridges is the estimation of component capacity, namely the quantification of *limit state* (damage state) *thresholds*. According to the basic principles of the methodology proposed, limit state thresholds should be component-specific, additionally accounting for the specific properties of the retrofit measure. It is noted that the present paper focuses on the most critical component of bridges, namely bridge piers; data for limit state thresholds for bearings and abutments can be found elsewhere (Stefanidou, (2016), Stefanidou and Kappos (2015)).
Since both as-built pier core and jacket properties should be considered for limit state thresholds' quantification, a database for cylindrical (and hollow cylindrical) piers retrofitted with R/C and FRP jackets is created, assuming a broad range of varying core and jacket parameters (Figure 1). The latter include pier geometry, axial load, material strength, reinforcement properties, and jacket thickness and properties; the database is created considering all possible combinations.

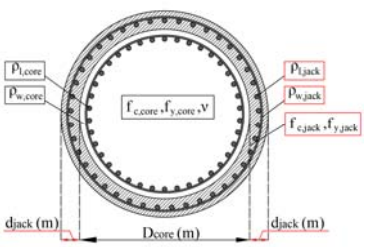

Parameters	Values		
D_{core} (m)	1.50	2.0	–
ν	0.15	0.30	–
$\rho_{l,core}$	0.005	0.020	–
$\rho_{w,core}$	0.0075	0.012	–
$f_{c,core}$ (MPa)	16	25	30
$f_{y,core}$ (MPa)	220	400	500
d_{jack} (m)	0.10	0.20	0.30
$\rho_{l,jacket}$	0.01	0.025	
$\rho_{w,jacket}$	0.009	0.015	
$f_{c,jacket}$ (MPa)	30	40	45
$f_{y,jacket}$ (MPa)	500	–	–
All possible combinations ***N=5184***			

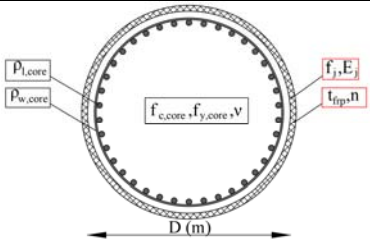

Parameters	Values		
D_{core} (m)	1.50	1.80	2.0
ν	0.15	0.30	–
$\rho_{l,core}$	0.005	0.020	–
$\rho_{w,core}$	0.0075	0.012	–
$f_{c,core}$ (MPa)	16	25	30
$f_{y,core}$ (MPa)	220	400	500
t_{FRP} (mm)	0.3	0.5	0.8
n (number of layers)	1	3	5
E_j (MPa)	225000	75000	
f_j(MPa)	4150	2450	–
All possible combinations ***N=3888***			

Figure 1. Parameters considered for cylindrical piers retrofitted with R/C and FRP jackets

Limit state thresholds are initially qualitatively and quantitatively defined using *local* EDPs, namely the (R/C or FRP) retrofitted section's curvature related to the material strains developed (Table 1). For the quantitative definition of the four limit states considered, material strain limits based on literature recommendations and relevant experimental results are used (Lu et al., (2005), Sheikh and Legeron, (2010), Priestley et al., (2007), Mirmiran and Shahawy, (1997)). Subsequently, moment-curvature analysis of the pier cross sections is performed and the curvature value at the step that material strain limits (listed in Table 1) are exceeded is recorded (φ_1, φ_2, φ_3, φ_4).

At this point it should be noted, that for the case of retrofitted piers (with R/C and FRP jackets), additional failure modes should be considered, compared to as-built sections. In particular, for piers retrofitted with R/C jackets, the possibility that the ultimate deformation is exceeded in the concrete core before the jacket, should be accounted for. It is however noted that the latter happens rarely and for jacket thicknesses up to 10cm. Local EDPs (and hence the capacity) of retrofitted sections are strongly affected by the model of confined concrete (R/C or FRP jacket) adopted for moment-curvature analysis. The key parameter that should be accounted for during model selection is the consideration of core confinement, affecting the ultimate stress and deformation. For example, for the case of R/C jacketed piers, consideration of core confinement results in substantial increase of confinement efficiency ('double' core confinement, Ong *et al.*, 2004). For the case of FPR-confined concrete, a large number of available confinement models ignore core confinement, while in some cases, simultaneous consideration (superposition) of confinement due to core transverse reinforcement and FRP is suggested. However, Biskinis and Fardis, (2013) suggested that the above is not accurate, since core confinement is activated subsequent to FRP rupture. Regarding the estimation of ultimate curvature and failure for the case of piers retrofitted with FRP jacket, increased effectiveness due to initial core confinement is proposed, according to the following (Biskinis and Fardis, 2013):

- Estimation of ultimate curvature and failure assuming confinement due to the FRP jacket only.
- Estimation of ultimate curvature and failure of the core, assuming confinement due to transverse reinforcement only (after FRP rupture). If the core's flexural capacity is greater than 80% of that corresponding to confinement due to FRP jacketing only, the ultimate core deformation is assumed to be reached later.

Table 1. Limit state thresholds of retrofitted piers in terms of local EDP

Limit State (LS)	Threshold values of curvature (φ)	Quantitative Performance Description
LS 1 – Minor-Slight damage	$\boldsymbol{\varphi_1}$: φ_y	Quasi-elastic behaviour – Cracks barely visible.
LS 2 – Moderate damage	$\boldsymbol{\varphi_2}$: min (φ: $\varepsilon_c > 0.004$, φ: $\varepsilon_s \geq 0.015$)	Spalling of the cover concrete; strength may continue to increase – Crack width 1-2mm.
LS 3 – Major-Extensive damage	$\boldsymbol{\varphi_3}$: min (φ: $\varepsilon_c \leq 0.004 + 1.4 \cdot \rho_w \cdot \frac{f_{yw}}{f_{cc}}$, φ: $\varepsilon_s \geq 0.06$)	First hoop fracture, buckling of longitudinal reinforcement, initiation of crushing of concrete core – Crack width>2mm.
LS 4 – Failure-Collapse	$\boldsymbol{\varphi_4}$: min (φ: $M < 0.90 \cdot M_{max}$, φ: $\varepsilon_s \geq 0.075$)	Loss of load-carrying capacity - patches of white began to show, plastic flow of resin, FRP rupture-Collapse

Based on the above, moment-curvature analysis is performed for the retrofitted sections included in the database (all possible combinations of parameters shown in Figure 1); moment-curvature (M-φ) curves and thresholds in curvature terms (φ_1, φ_2, φ_3, φ_4) are obtained. Since the methodology proposed for the calculation of bridge-specific fragility curves considers multiple critical components, the use of *global* EDPs (i.e. displacement of component control point) is suggested, relating local to global damage. To this end, inelastic (pushover) analysis of retrofitted piers is performed, considering cantilever column model with concentrated plasticity, to obtain limit state thresholds in displacement terms (Figure 2). The calculated moment-curvature curves are used as input at plastic hinge locations; details regarding the plastic hinge length calculation can be found elsewhere (Stefanidou and Kappos, 2017). A broad range of pier heights (5~20m) is considered and pushover analysis is performed taking into account P-delta effects. The displacement of the cantilever tip (d_i) at the instant that the deformation of the plastic hinge exceeds limit state thresholds (φ_1, φ_2, φ_3, φ_4), is recorded, using ad-hoc software developed in Matlab, additionally considering shear failure modes; d_1, d_2, d_3, d_4 are then derived. In particular, the shear demand at each step is compared to the ultimate shear capacity V_u and the associated displacement value

is recorded and compared to the one derived considering flexural failure. Threshold values in displacement terms depend on the boundary conditions (pier-to-deck connection and foundation type); therefore, the displacement of the equivalent cantilever is related to that of the restrained pier as described in Figure 2 and, in more detail, in Stefanidou and Kappos, (2017).

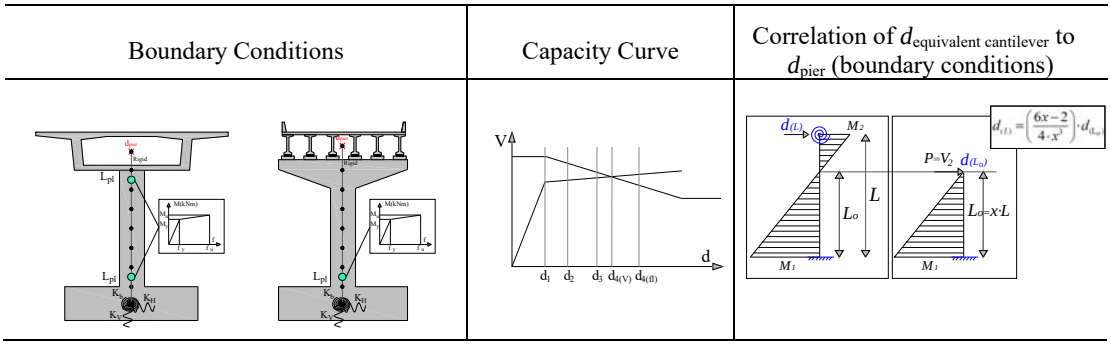

Figure 2. Calculation of limit state thresholds in displacement terms (global engineering demand parameter)

All retrofitted sections (R/C and FRP jackets) are paired with the considered range of pier heights (5~20m), inelastic cantilever models are created, and pushover analyses are performed for the calculation of limit state thresholds in displacement terms (d_1, d_2, d_3, d_4). Analysis results are processed using the advanced least squares method for linear equality constraints and empirical relationships are proposed for the calculation of limit state thresholds of retrofitted piers, relating as-built and retrofitted values, as presented in Table 2 for the case of cylindrical piers retrofitted with R/C and FRP jackets.

Table 2. Limit state thresholds of retrofitted piers in terms of local EPD

Cylindrical Piers (RC Jacket)

$$(\delta_{RCj}/\mathrm{H})/(\delta_{core}/\mathrm{H}) = \beta_0 + \beta_1\cdot(D_{RCj}/D_{core}) + \beta_2\cdot(\rho_{l,RCj}/\rho_{l,\mathrm{core}}) + \beta_3\cdot(\rho_{\mathrm{w},RCj}/\rho_{w,core}) + \beta_4\cdot(f_{c,RCj}/f_{c,core}) + \beta_5\cdot(f_{\mathrm{y},RCj}/f_{\mathrm{y},core})]$$

	β_0	β_1	β_2	β_3	β_4	β_5
$(\delta_{1,RCj}/\mathrm{H})/(\delta_{1,core}/\mathrm{H})$	+0.566	+0.059	+0.129	+0.016	-0.169	+0.399
$(\delta_{2,RCj}/\mathrm{H})/(\delta_{2,core}/\mathrm{H})$	+1.167	-0.353	+0.012	+0.007	+0.002	+0.164
$(\delta_{3,RCj}/\mathrm{H})/(\delta_{3,core}/\mathrm{H})$	+0.802	-0.212	-0.013	+0.219	-0.324	+0.528
$(\delta_{4,RCj}/\mathrm{H})/(\delta_{4,core}/\mathrm{H})$	+1.094	-0.274	+0.003	+0.124	-0.334	+0.388

Cylindrical Piers (FRP Jacket)

$$(\delta_{FRPj}/\mathrm{H})/(\delta_{core}/\mathrm{H}) = \beta_0 + \beta_1\cdot(D_{FRP,j}/D_{core}) + \beta_2\cdot(E_{FRP,j}/E_{c,core}) + \beta_3\cdot(f_{jFRP,j}/f_{c,core}) + \beta_4\cdot(\rho_{fFRP,j}/\rho_{w,core})$$

	β_0	β_1	β_2	β_3	β_4
$(\delta_{1,FRPj}/\mathrm{H})/(\delta_{1,core}/\mathrm{H})$	-1.27e+02	+1.28e+02	-9.14e-03	+4.06e-03	+4.89e-02
$(\delta_{2,FRPj}/\mathrm{H})/(\delta_{2,core}/\mathrm{H})$	-7.610	+8.580	+2.67e-03	+4.49e-04	2.91e-02
$(\delta_{3,FRPj}/\mathrm{H})/(\delta_{3,core}/\mathrm{H})$	+9.02e+01	-8.96e+01	-1.07e-01	+1.40e-02	+4.71e-01
$(\delta_{4,FRPj}/\mathrm{H})/(\delta_{4,core}/\mathrm{H})$	+7.56e+01	-7.49e+01	-7.61e-02	+1.11e-02	+4.02e-01

Using the aforementioned empirical relationships, the effect of varying as-built and retrofitted parameters on seismic capacity (limit state thresholds) can be easily assessed. For example, the effect of different reinforcement ratios and material strengths on displacement ductility ratio, is illustrated in

Figure 3 for the case of cylindrical piers retrofitted with R/C and FRP jacket. Regarding the R/C jacketed piers, it is noted that the effect of transverse reinforcement on displacement ductility is greater than the relevant of longitudinal reinforcement, whereas for the FRP jacketed piers, the confinement effectiveness is the most critical parameter. Based on the above, the empirical relationships can be further used for the preliminary selection and effectiveness evaluation of the retrofit measure on pier capacity.

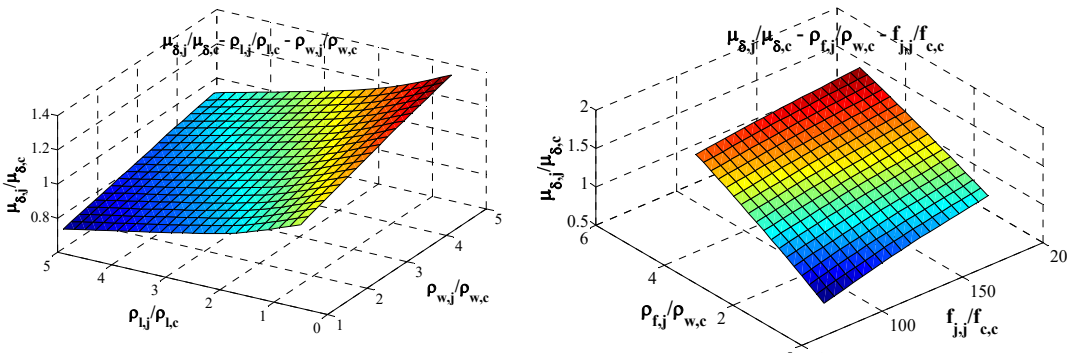

D_j=2.4 (m) , D_c=2.0 (m) , $f_{c,j}$= 38 (MPa), $f_{c,c}$= 28 (MPa), $f_{y,j}$= 550 (MPa), $f_{y,c}$= 440 (MPa)

Dj=2.001 (m), Dc=2.0 (m), Ef,j=225000 (MPa), fc,c=28 (MPa)

Figure 3. Effect of various parameters on displacement ductility of as-built and retrofitted piers (retrofit with R/C(left) and CFRP(right) jacketing)

Capacity thresholds for the four limit states considered (minor, major, extensive damage and collapse) are depicted in Figure 4, for the case of cylindrical piers in terms of dimensionless global EDPs, namely displacement ductility (μ_d) and drift (d/h). The variability in limit state thresholds, that depends on both pier type and the retrofit measure, is evident; therefore, a uniform value for the threshold may either overestimate or underestimate component capacity. It should be emphasised that Figure 4 shows mean values, calculated by means of inelastic analysis of components included in the database, having a specific range of different parameters (geometry, material, reinforcement ratio and normalised axial load for each pier type).

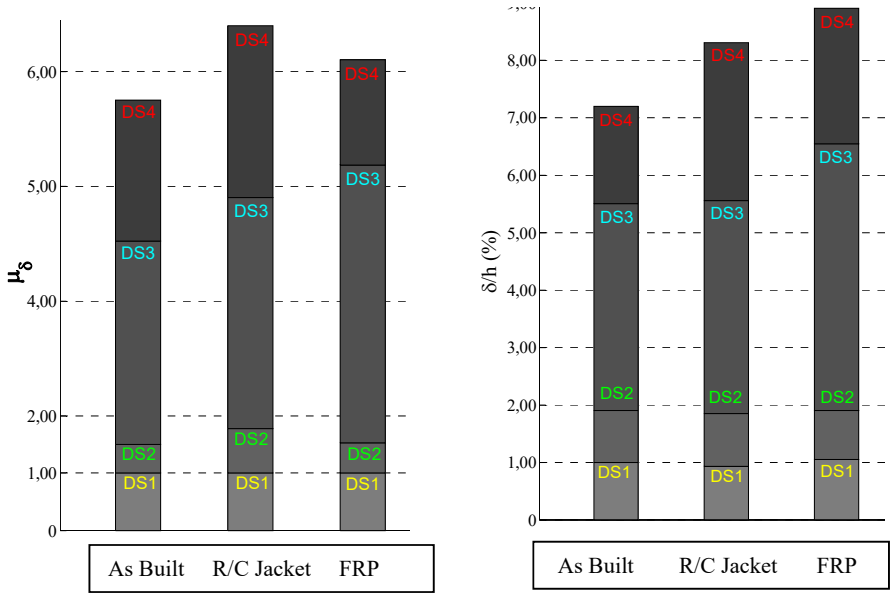

Figure 4. Limit state thresholds of retrofitted bridge piers (R/C and FRP jackets) in terms of displacement ductility (μ_δ) and drift (d/h %)

Uncertainty in capacity is also estimated, assuming proper distributions of random variables (material strengths, ultimate strain ε_{cu}, and plastic hinge length L_{pl}), with mean and standard deviation values, as described in Stefanidou and Kappos (2015). Latin Hypercube sampling is used with 100 realizations of each retrofitted member, analysis results are processed, and dispersion (β_c) values are proposed for each different retrofit technique (Table 3).

Table 3. Uncertainty in capacity of retrofitted piers

Retrofit measure	$\beta_{c,\,L.S.1}$	$\beta_{c,\,L.S.2}$	$\beta_{c,\,L.S.3}$	$\beta_{c,\,L.S.4}$	$\beta_{c,mean}$
R/C Jacket	0.17	0.28	0.37	0.41	0.31
FRP Jacket	0.10	0.32	0.46	0.52	0.35

4. SEISMIC DEMAND, RELATED UNCERTAINTIES AND DERIVATION OF BRIDGE-SPECIFIC FRAGILITY CURVES

According to the methodology proposed herein, so long as component-specific threshold limit state values (capacity) and the associated uncertainty are defined, the demand at the control point of every (as-built or retrofitted) component has to be estimated, in order to derive fragility curves for each limit state. Uncertainty in demand is defined based on the results of detailed structural models and nonlinear analysis of retrofitted representative bridge types (according to the classification scheme described in Stefanidou and Kappos, 2015). Uncertainty in material properties, gap size (at the abutment), bearing stiffness and site properties are considered during analysis of representative bridges. As noted previously, reduced Monte Carlo simulation for N=100 samples is used and incremental dynamic analysis for selected accelerograms scaled to different levels of earthquake intensity is performed in order to calculate β_d for the relevant bridge class.

A Probabilistic Seismic Demand Model (PSDM) is used to estimate the dispersion value, representing the uncertainty in demand. It is recalled here that there are two approaches regarding the implementation of the PSDM, namely the "cloud" (Probabilistic Seismic Demand Analysis) and the "scaling" (Incremental Dynamic Analysis) approach, the latter having the advantage of not requiring an a priori assumption for the probabilistic distribution of seismic demand for fitting fragility curves (Zhang and Huo, 2009). The approach implemented herein is IDA for different levels of seismic action (typically ranging from 0.1g to 1.0g). The limit state probability of exceedance at a specific intensity I_M level equals the occurrence ratio of the specific limit state, defined as the ratio of the number of damage cases n_i, for the damage state i over the number of simulations *N*, i.e.

$$P[(\mathrm{D} \geq \mathrm{DS}_i \,|\, I_M) = \frac{n_i}{N} \quad (\mathrm{i} = 1 to 4) \tag{1}$$

$$P[(\mathrm{D} \geq \mathrm{LS} \,|\, I_M) = \int_{-\infty}^{I_M} \frac{1}{I_M \cdot \sqrt{2\pi \cdot \hat{\beta}}} \cdot e^{\left\{ -\frac{[\ln(I_M) - \hat{\mu}]}{2 \cdot \hat{\beta}^2} \right\}} d(\mathrm{I}_M) \tag{2}$$

Logarithmic standard deviation β_D is calculated for every bridge component (piers, bearings, abutments) based on the results of nonlinear response-history analysis of all the realizations considered and different levels of A_g. Mean and standard deviation values are obtained from equations 3 and 4, where *M* is the number of realizations and a_i is associated with the onset of collapse for the i^{th} realization (Porter et al., 2007).

$$\hat{\mu} = \frac{1}{\mathrm{M}} \cdot \sum_{i=1}^{\mathrm{M}} \ln(a_i) \tag{3}$$

$$\hat{\beta}_D = \sqrt{\frac{1}{(M-1)} \cdot \sum_{i=1}^{M} (\ln(a_i) - \hat{\mu})^2} \quad (4)$$

The total uncertainty is estimated for every component according to equation 5, under the assumption of statistical independence (discussed in Stefanidou and Kappos, 2017)

$$\beta_{tot} = \sqrt{\beta_C^2 + \beta_D^2 + \beta_{LS}^2} \quad (5)$$

Finally, bridge-specific fragility curves are calculated on the basis of the above (mean and standard deviation values), assuming series connection between components (equation 6) except for LS4 corresponding to bridge collapse and related to collapse of bridge piers only.

$$P(F_{br}) = 1 - \prod_{i=1}^{m} [1 - P(F_i)] \quad (6)$$

Where
i : Bridge components considered; namely bridge piers, bearings, abutments
P(F_{br}): Probability of bridge failure
P(F_{br}): Probability of component failure

5. CASE STUDY BRIDGE

A typical overpass of Egnatia Motorway, N. Greece (Figure 6) having cylindrical piers monolithically connected to the deck that consists of a prestressed concrete box section, was retrofitted using different strategies, namely R/C and FRP jackets, with varying properties and bridge-specific fragility curves were derived. According to Gkatzogias and Kappos (2015), the piers of the case study bridge were overdesigned, therefore reduced (compared to the as-built bridge) diameter and longitudinal and transverse reinforcement ratios are assumed (Table 4). Definition of limit states and quantification of limit state thresholds (capacity) of the retrofitted bridge piers were calculated according to §3. The effect of different retrofit measures, varying R/C jacket parameters (jacket thickness and longitudinal reinforcement ratio) and varying FRP properties (carbon and glass FRP) on bridge fragility are studied and discussed. Since system fragility is calculated considering series connection between critical components, the effectiveness of retrofit measures and strategies should be assessed at both system and component level.

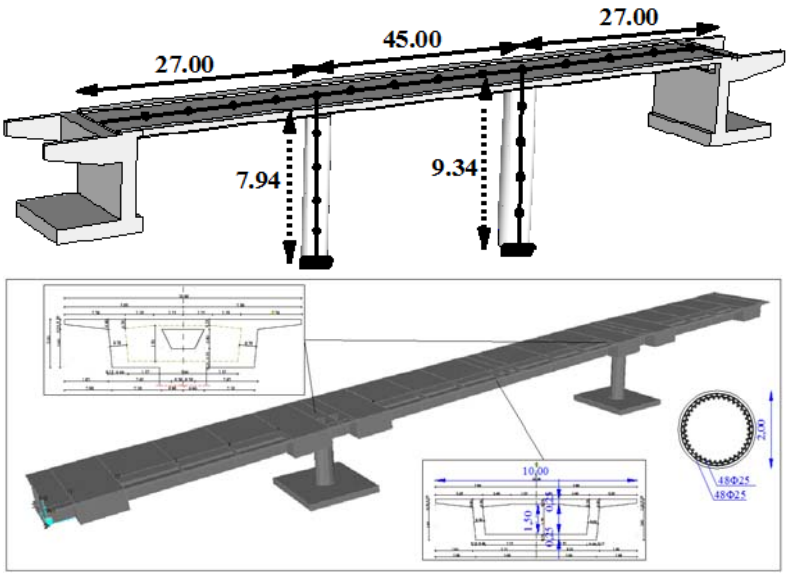

Figure 6. Case study of an Egnatia Motorway Overpass

Table 4. Variation of parameters of retrofitted piers (R/C jacket)

Parameters	**As-built (AB)**	**RC Jacket (RCJ)**	**RCJ(A)**	**RCJ(B)**
D (m)	1.50	1.90	1.9	**2.1**
$f_{c,m}$ (MPa)	24 (C 16/20)	28 (C 20/25)	28 (C 20/25)	28 (C 20/25)
f_y (MPa)	440 (S400s)	550 (B 500c)	550 (B 500c)	550 (B 500c)
ρ_l	0.0102	0.015	**0.025**	0.015
ρ_w	0.004	0.011	0.011	0.011

Fragility curves for as-built and retrofitted bridge, namely the probability that bridge damage exceeds a specific limit state threshold (Demand > Capacity) for different levels of earthquake intensity (PGA), are depicted in Figures 7 and 8. It is emphasised that limit state thresholds of retrofitted piers (capacity) are component-specific, calculated using the empirical relationships proposed herein, accounting for the effect of as-built and retrofitted section properties.

As shown in Figure 7 (left), both R/C and FRP jackets resulted in reduced seismic fragility of the system, mainly with regard to higher limit states, due to core confinement and ductility enhancement. It should be pointed out that R/C jackets may result in fragility *increase* for the first limit state (longitudinal direction, LS1, related to φ_y), owning to the lower, compared to the as-built, yielding curvature of the R/C jacketed pier. The effectiveness of R/C jacketing is higher, compared to FRP jacketing, for the lower limit states; however, this is not the case for higher limit states, since confinement with FRP jacket results in more effective ductility enhancement. In particular, the reduce in seismic fragility for LS2 is up to 35% for the case of R/C jacketed piers and 25% for the case of piers retrofitted with FRP jackets, whereas for LS3 the relevant reduce is 40% and 47% respectively.

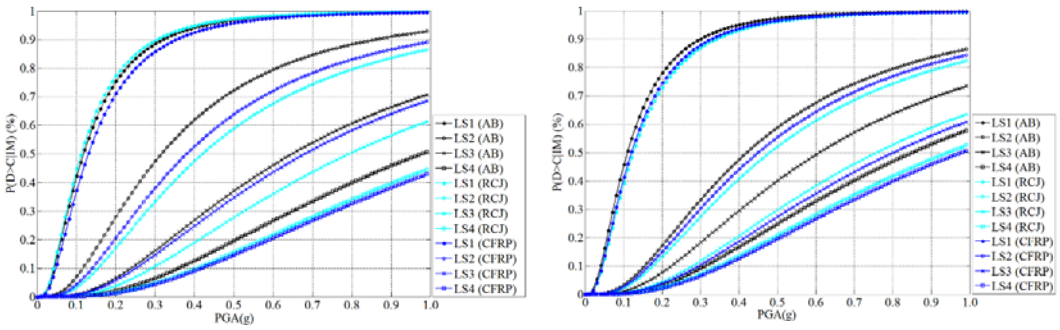

Figure 7. Fragility curves of the as-built (AB) and retrofitted with RC (RCJ) and FRP (CFRP) jacket bridge (longitudinal (left) and transverse (right) direction)

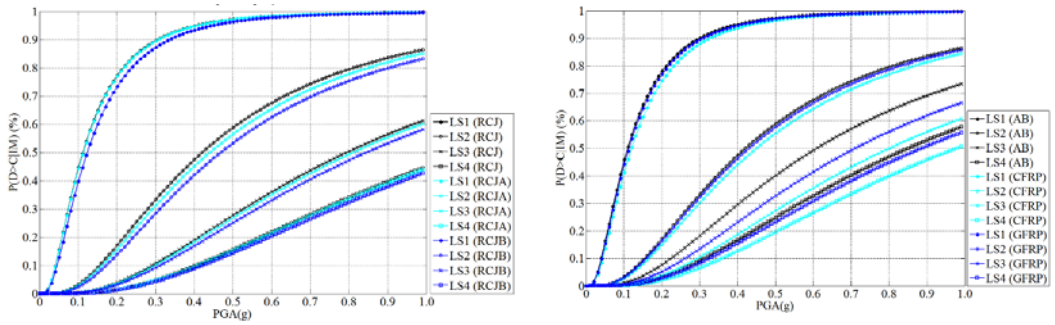

Figure 8. Fragility curves of the longitudinal direction retrofitted with RC jackets (RCJ, RCJA, RCJB) (left) and the transverse direction retrofitted with FRP jackets (CFRPandGFRP)

Fragility analysis results for the case study retrofitted bridge, indicated that both increase in longitudinal reinforcement ratio and jacket thickness resulted in reduced seismic fragility (Figure 8, left). Based on parametric analysis results, the fact that increase in stiffness (jacket thickness) is slightly more effective than increase in strength (reinforcement ratio) for seismic fragility reduction was outlined. Regarding the case of FRP-jacketed piers (Figure 8, right) and their effect on bridge fragility it should be noted that both CFRP and GFRP resulted in reduced fragility, mainly for higher limit states. However, retrofit with CFRPs was in general more effective, regarding seismic fragility reduction for all limit states considered, compared to GFRPs.

The conclusions reached and presented above, could be used for selection of the optimum retrofit measure for the bridge type considered. However, it should be stressed that the optimum selection should be additionally related to the target performance level, as depicted in Figure 9.

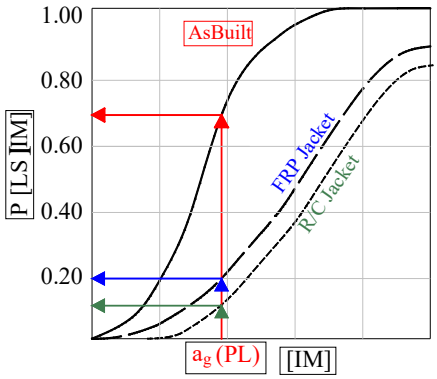

Figure 9. Optimum selection of retrofit measure according to the selected performance level

In order to highlight the effect of component-specific limit state thresholds on fragility analysis of retrofitted (with R/C and FRP jackets) bridges, fragility curves were derived for the limit states considered (LS1-LS4), based on the proposed component-based methodology and on HAZUS recommendations (limit state thresholds proposed by Mander and Basöz, 1999). As depicted in Figure 10, for both cases (R/C and FRP jacket), HAZUS was found to underestimate the failure probability for the first two limit states, rendering the results unconservative. However, it should be noted that fragility curves for higher limit states, calculated according to HAZUS recommendations are in good agreement with the corresponding curves derived according to the proposed methodology.

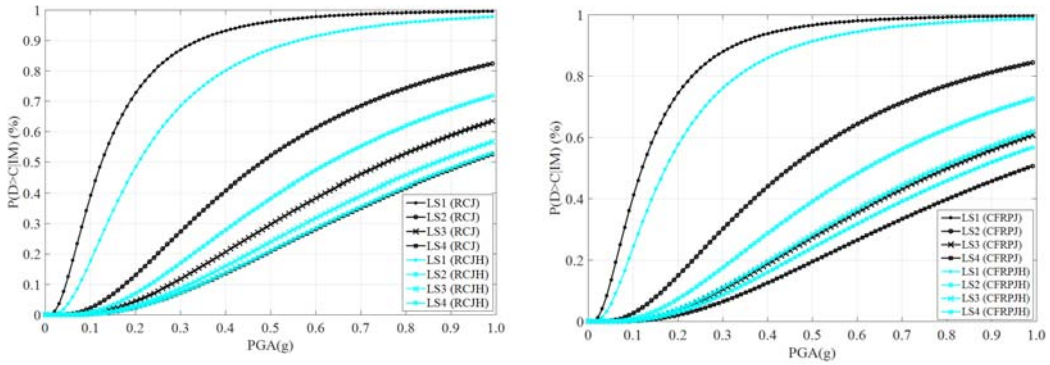

Figure 10. Fragility curves of the bridge piers retrofitted with RC (left) and CFRP (right) jackets considering component-based limit state thresholds according to the proposed methodology (RCJ, CFRP) and HAZUS recommendations (RCJH, CFRPH)

6. CONCLUSIONS

The present study highlighted the effect of component-specific limit state definition in fragility analysis of retrofitted bridges and provided insight into the effect of varying retrofit measure properties on bridge fragility, the optimum selection of retrofit measure, and comparison with HAZUS recommendations. The main conclusions reached are summarised below:

- Pier jacketing (R/C or FRP) results in seismic fragility reduction for higher limit states and both bridge directions, owning to core confinement and the increase in ultimate concrete strain (ε_{cu}).
- R/C jackets may result in fragility increase for the first limit state (LS1, related to φ_y), owning to the lower, compared to the as-built, yielding curvature of the R/C jacketed pier.
- Retrofit with R/C jackets is more effective, compared to FRP wrapping, for fragility reduction in LS2 and LS3; however, this is not the case for the upper limit states. The latter is mainly due to the fact that confinement with FRP jacket results in more effective ductility enhancement.
- For both cases (R/C and FRP jacket), derived fragility curves according to HAZUS were found to underestimate the failure probability for the first two limit states, rendering the results unconservative; however, the match was satisfactory for the two higher limit states.

7. ACKNOWLEDGEMENTS

This research has been co-financed by the European Union (European Social Fund – ESF) and Greek national funds through the Operational Programme "Education and Lifelong Learning" of the National Strategic Reference Framework (NSRF) – Research Funding Program: ARISTEIA II: Reinforcement of the interdisciplinary and/or interinstitutional research and innovation.

8. REFERENCES

Biskinis D, Fardis M N (2013). Models for FRP-wrapped rectangular RC columns with continuous or lap-spliced bars under cyclic lateral loading. *Engineering Structures*, 57: 199–212.

Gkatzogias K., Kappos A. (2015). Performance-based seismic design of concrete bridges. *SECED 2015 Conference: Earthquake Risk and Engineering towards a Resilient World*. Cambridge, UK.

Kim S.-H., Shinozuka M. (2004). Development of fragility curves of bridges retrofitted by column jacketing. *Probabilistic Engineering Mechanics*, 19(1-2): 105–112.

Lu Y, Gu X, Guan J. (2005). Probabilistic Drift Limits and Performance Evaluation of Reinforced Concrete Columns. *Journal of Structural Engineering, ASCE*, 131(6): 966–978.

Mander J, Basöz N. (1999). *Enhanchement of the Highway Transportation Lifeline Module in HAZUS*. Final Pre-Publication Draft (#7) prepared for National Institute of Building Sciences (NIBS).

Mirmiran A, Shahawy M. (1997). Behavior of Concrete Columns Confined by Fiber Composites. *Journal of Structural Engineering, ASCE*, 123(5): 583–590.

Nielson BG (2005). Analytical Fragility Curves for Highway Bridges in Moderate Seismic Zones Analytical Fragility Curves for Highway Bridges in Moderate Seismic Zones. *PhD Thesis*, Georgia Institute of Technology, Atlanta

Ong KCG, Kog, YC, Yu, CH, Sreekanth, APV (2004). Jacketing of reinforced concrete columns subjected to axial load. *Magazine of Concrete Research*, 56(2), 89–98.

Padgett JE, DesRoches R (2009). Retrofitted Bridge Fragility Analysis for Typical Classes of Multispan Bridges. *Earthquake Spectra*, 25(1):117-141.

Sheikh N, Legeron F (2010). Seismic performance-based design of bridges with quantitative local performance criteria. *2nd International Structures Speciality Conference*. Winnipeg, Manitoba.

Stefanidou SP (2016). Structure-specific Fragility Curves for As-Built and Retrofitted Bridges. *PhD Thesis*, Aristotle University of Thessaloniki.

Stefanidou SP, Kappos AJ (2013). Optimum Selection Of Retrofit Measures For R/C Bridges Using Fragility Curves. *4th ECCOMMAS Thematic Conference on Computational Methods in Structural Dynamics and Earthquake Engineering*. Kos Island, Greece.

Stefanidou SP, Kappos, AJ (2015). Efficiency of different retrofit measures in reducing seismic fragility of bridges. *16th European Bridge Conference,* Edinburgh, UK.

Stefanidou SP, Kappos AJ (2017). Methodology for the development of bridge-specific fragility curves. *Earthquake Engineering and Structural Dynamics*, 46: 73–93.

Towashiraporn P (2004). Building Seismic Fragilities using Response Surface Metamodels. *PhD Thesis*, Georgia Institute of Technology.

Zhang J, Huo Y (2009). Evaluating effectiveness and optimum design of isolation devices for highway bridges using the fragility function method. *Engineering Structures*, 31(8), 1648–1660.